

General Disclaimer

One or more of the Following Statements may affect this Document

- This document has been reproduced from the best copy furnished by the organizational source. It is being released in the interest of making available as much information as possible.
- This document may contain data, which exceeds the sheet parameters. It was furnished in this condition by the organizational source and is the best copy available.
- This document may contain tone-on-tone or color graphs, charts and/or pictures, which have been reproduced in black and white.
- This document is paginated as submitted by the original source.
- Portions of this document are not fully legible due to the historical nature of some of the material. However, it is the best reproduction available from the original submission.

AD-783 679

PIONEER X: OBSERVATIONS OF ENERGETIC
ELECTRONS IN THE JOVIAN MAGNETOSPHERE

B. A. Randall

Iowa University

Prepared for:

Office of Naval Research
National Aeronautics and Space Administration

June 1974

DISTRIBUTED BY:

NTIS

National Technical Information Service
U. S. DEPARTMENT OF COMMERCE
5285 Port Royal Road, Springfield Va. 22151

UNCLASSIFIED

SECURITY CLASSIFICATION OF THIS PAGE (When Data Entered)

AD 783 679

REPORT DOCUMENTATION PAGE		READ INSTRUCTIONS BEFORE COMPLETING FORM
1. REPORT NUMBER U. of Iowa 74-26 ✓	2. GOVT ACCESSION NO.	3. RECIPIENT'S CATALOG NUMBER
4. TITLE (and Subtitle) PIONEER X: OBSERVATIONS OF ENERGETIC ELECTRONS IN THE JOVIAN MAGNETOSPHERE ✓		5. TYPE OF REPORT & PERIOD COVERED Progress June 1974
7. AUTHOR(s) B. A. Randall		6. PERFORMING ORG. REPORT NUMBER
9. PERFORMING ORGANIZATION NAME AND ADDRESS Department of Physics and Astronomy The University of Iowa Iowa City, Iowa 52242 ✓		8. CONTRACT OR GRANT NUMBER(s) N00014-68-A-0196-0009 ✓
11. CONTROLLING OFFICE NAME AND ADDRESS Office of Naval Research Arlington Virginia 22217		10. PROGRAM ELEMENT, PROJECT, TASK AREA & WORK UNIT NUMBERS
14. MONITORING AGENCY NAME & ADDRESS (if different from Controlling Office)		12. REPORT DATE June 1974
		13. NUMBER OF PAGES 43
		15. SECURITY CLASS. (of this report) UNCLASSIFIED
		16a. DECLASSIFICATION / DOWNGRADING SCHEDULE
16. DISTRIBUTION STATEMENT (of this Report) Approved for public release; distribution is unlimited.		
17. DISTRIBUTION STATEMENT (of the abstract entered in Block 20, if different from Report)		
18. SUPPLEMENTARY NOTES Presented to the Neil Brice Memorial Symposium on Magnetospheres, Frascati, Italy, May 28 through June 1, 1974		
19. KEY WORDS (Continue on reverse side if necessary and identify by block number) Jupiter Planetary Magnetospheres Radiation Belts		
20. ABSTRACT (Continue on reverse side if necessary and identify by block number) [See page following.] Reproduced by NATIONAL TECHNICAL INFORMATION SERVICE U S Department of Commerce Springfield VA 22151		

43

DD FORM 1 JAN 73 1473

EDITION OF 1 NOV 65 IS OBSOLETE
S/N 0102-014-6601

UNCLASSIFIED

SECURITY CLASSIFICATION OF THIS PAGE (When Data Entered)

A survey has been made of the spatial and angular distributions and energy spectra of energetic electrons in the magnetosphere of Jupiter. In the hard trapping region $r < 20 R_J$, the distribution of electrons $E_e > 21$ MeV is

$$J_0 \text{ (cm}^2 \text{ sec)}^{-1} = 3.0 \times 10^8 \exp(-L/1.45) \left(\frac{\cos^6 \Lambda}{\sqrt{4 - 3 \cos^2 \Lambda}} \right)^{m/2}$$

where $m = 3.5 + (3.86/L)^8$,

r = radial distance in Jovian radii (R_J),

Λ = magnetic latitude for a centered dipole with a tilt of

9.5° towards 230° System III longitude, and

$$L = r / \cos^2 \Lambda.$$

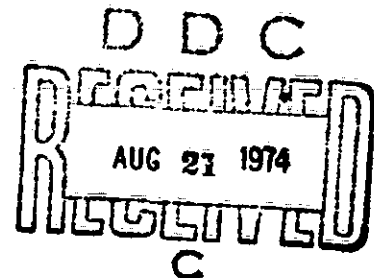
The equatorial differential energy spectrum for electrons with energy greater than 21 MeV is $dJ/dE(E, r) \approx 10^{12} E^{-3.5} \exp(-r/1.45)$ per $\text{cm}^2\text{-sec-MeV}$.

The outer magnetosphere ($r > 20 R_J$) appears to be a quasi-trapping disc-like region, possibly similar in some respects to the magnetotail of the earth. The axial thickness of this region is only a few R_J but its radial extent is about $100 R_J$ on the sunward side and much larger on the dawn side. This region seems to be the source of emission of energetic protons and electrons into interplanetary space.

PIONEER X: OBSERVATIONS OF ENERGETIC
ELECTRONS IN THE JOVIAN MAGNETOSPHERE

by

B. A. RANDALL



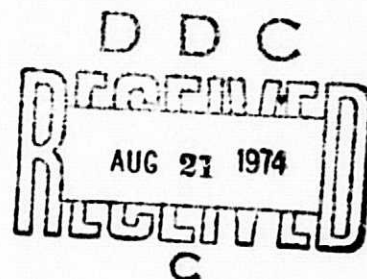
Department of Physics and Astronomy
The University of Iowa
Iowa City, Iowa 52242 USA

Presented to the Neil Brice Memorial Symposium on Magneto-
spheres, Frascati, Italy, May 28 through June 1,
1974.

PIONEER X: OBSERVATIONS OF ENERGETIC
ELECTRONS IN THE JOVIAN MAGNETOSPHERE

by

B. A. RANDALL



Department of Physics and Astronomy
The University of Iowa
Iowa City, Iowa 52242 USA

Presented to the Neil Brice Memorial Symposium on Magneto-
spheres, Frascati, Italy, May 28 through June 1,
1974.

I. INTRODUCTION

The University of Iowa experiment on Pioneer 10 is a simplified version of the originally proposed instrument. This simplification was due to the constraints specified by the National Aeronautics and Space Administration at the time of acceptance of the experiment. The reduced observational objectives of the experiment were:

- (a) To make an exploratory survey of the intensities, energy spectra, and angular distribution of energetic particles in the magnetosphere of Jupiter;
- (b) To measure the heliocentric radial gradient of the intensity of galactic cosmic rays $E_p \geq 80$ MeV [Van Allen, 1972, 1973; Thomsen, 1974]; and
- (c) To study the occurrence, intensity, and angular distribution of solar flare particles and their propagation through the interplanetary medium at large heliocentric distances.

A preliminary report of our Jovian encounter measurements has been published [Van Allen et al., 1974a]. The present paper represents a continuing analysis of those data.

II. DESCRIPTION OF INSTRUMENT

The design of the experiment was guided by the theoretical interpretation by Chang and Davis [1962], Thorne [1963, 1965], and Ortwein et al. [1966] of the observed decimetric radio emission from Jupiter. The observations are reviewed by Carr and Gulkis [1969]. The theoretical predictions indicated that Jupiter is encircled by a very high intensity of relativistic, trapped electrons.

Previous observational experience with trapped relativistic electrons produced by Starfish in 1962 [Van Allen et al., 1963] also served as a guide in the design. The design objectives were that the instrument should be able to make significant determinations of the intensity of energetic electrons and yet have a very large dynamic range in intensity and be simple, rugged, and very reliable for many years. The instrument should also be insensitive to radiation damage and temperature.

The basic detectors were seven miniature Geiger-Mueller tubes. Four were the EON 6213 type, many of which have been flown on many missions since Pioneer III (1958 θ), and the other three were EON 5107's. The latter type had never been flown before but had proved, with stringent selection and testing, to equal the EON 6213 in reliability and to have a much larger dynamic range.

The seven tubes were in three different physical arrangements. Three EON 6213's (A, B, and C) were mounted in a single block as shown in Figure 1. Detector C is in the center and is omnidirectionally shielded. Detectors A, B, and C are similarly shielded on the sides but A and B have thin unidirectional collimators in the +X direction. Each detector is sampled separately; also double (AB) and triple (ABC) coincidences with a resolving time of 1 μ s are sampled.

The second assembly comprises an omnidirectionally shielded, triangular array of three EON 5107 tubes (D, E, F) as shown in Figure 2. The rate of D and the triple coincidence rate of DEF are sampled.

The third assembly, detector G, used an EON 6213 with a gold-plated scattering aperture. The purpose of the scatter arrangement was to combine the energy dependence of the scattering aperture and the higher proton threshold of the EON 6213, to obtain a hundredfold reduction in efficiency for non-penetrating protons compared with the efficiency for electrons. The physical arrangement for this detector is shown in Figure 3. The arrangement of the three within the University of Iowa experiment is shown in Figure 4.

The University of Iowa experiment uses 12 bits of each of the 192-bit main science frame. The signal processor, doubly redundant and switchable on command, uses two 24-bit accumulators which

are alternately being read out or accumulating. The 24-bits are compressed into 12 bits using a quasi-logarithmic scheme of counting the leading zero order bits, then transmitting this number and the leading significant bits. A complete cycle of University of Iowa data comprises eleven main science frames. This includes a sync word and two samples from G and ABC.

The accumulating period for each sample depends on the bit rate in the following manner: Period equals $192/\text{Bit Rate}$. The bit rate was selected by ground command and was 2^N where N was between 4 and 11. During the Jovian encounter the accumulation time was either 0.1875 or 0.375 sec from all real time data transmission. When the spacecraft was occulted by the planet, the data were stored at 16 bit per second on the spacecraft and subsequently played back.

The spacecraft was oriented such that the spin axis (+Z) was pointed continuously at the earth with an error of less than 1° . The University of Iowa experiment looks out along the +X axis. In our analysis the roll angle is measured from the ascending node of the spacecraft's equator on the ecliptic to the +X axis. Because of the non-integral relationship of the spacecraft's rotational period of 12.64 sec and the sampling period, successive samples are always made at different angles. Approximately 52 successive samples produce a complete roll angle distribution with about 7° between each sample.

Our instrument which has a total mass of 1.64 kg and power consumption of 0.78 watt has operated continuously for some 26 months with no abnormalities or malfunctions of any kind. This includes the Jovian encounter and postencounter period to date of writing.

III. THE MAGNETOSPHERE

The Pioneer 10 flyby showed that the radiation belts surrounding Jupiter can be separated into two distinct regions. The region outside of $20 R_J$, called the magnetodisc, is characterized by quasi-trapped particles in a magnetic field which does not rotate rigidly with the planet and deviates substantially from a dipolar field. Inside of $20 R_J$, the magnetic field becomes more dipolar and particles seem to be durably trapped.

To analyze the distribution of particle intensities it was necessary to find a coordinate system to organize the data. The best possibility under the circumstances seemed to be a comparison of the data using an L parameter [McIlwain, 1961]. To find the L value it is necessary to know the position and orientation of the dipole. The obvious choice was the model inferred by Smith et al. [1974] from the direct magnetometer measurements. Preliminary work had indicated that the intensities decreased approximately exponentially with radius and had a Gaussian dependence on magnetic latitude [Van Allen et al., 1974a]. The latter indicated that the equatorial pitch angle distribution could be represented by $\sin^m \alpha$. Figure 5 shows an example of the organization of the electron data $E > 21$ MeV by the model proposed by Smith et al. [1974]. There is a marked lack of the closure between inbound and outbound data beyond

$L > 7$ while the particle angular distributions indicate that the intensities should still be ordered beyond this region. The model inferred from decimetric and decametric radio observations [Mead, 1973] is a centered dipole tilted at 10° toward 224° System III longitude. This model worked much better than the previous one; but using a trial and error procedure, it was found that a better fit could be made for a centered dipole with a tilt of 9.5° towards 230° System III longitude. Figure 6 shows the particle intensity $E > 21$ connected to the equatorial intensity using an assumed angular distribution of $\sin^4 \alpha$ for this model. Figure 7 shows a similar plot using a more recent (13 May 1974) model proposed by Smith et al. This model does not organize the energetic particle data as well as the centered dipole with a tilt of 9.5° towards 230° longitude.

For the rest of this paper the model being used is a centered dipole with a tilt of 9.5° towards 230° System III longitude. The trial and error determination of these values indicated that a change of $\pm 0.5^\circ$ in tilt or $\pm 3^\circ$ longitude degraded the fit noticeably. The inbound and outbound data for detector C are shown on Figure 8 with no corrections. The exponential decrease of the equatorial data with L is clearly evident.

Examination of families of diagrams such as Figure 6 suggested that the loop inside L of 4 might be due to a monotonic increase in m with decreasing L . Detailed comparison of conjugate inbound and outbound data leads to the following expressions for m as a function

of L for detectors C and D. The L dependence of these coefficients is negligible for $L > 5$.

$$\text{For C: } m = 3.5 + (3.86/L)^8$$

$$\text{For D: } m = 4.0 + (5.567/L)^8$$

Both of these formulae are strictly empirical and there is no assurance that they are valid for lesser values of L . The results of this endeavor are clearly shown in Figures 9 and 10. The closure is very good for both curves and there is a definite tendency for both curves to roll over at closest approach. It is tempting to attribute this effect to a sweeping of particles by Amalthea. A theoretical analysis of phenomena would be useful in assessing validity of this suggestion. The Pioneer 11 spacecraft, which is now targeted for a periapsis of $1.6 R_J$, should also contribute to knowledge of this matter.

By least squares fitting to the data of Figures 9 and 10 in the range of $3.5 \leq L \leq 12 R_J$, we find

$$J(E_e > 21 \text{ MeV}) = 3.0 \times 10^8 \exp(-L/1.45) \left(\frac{\cos^6 \Lambda}{\sqrt{4 - 3 \cos^2 \Lambda}} \right)^{m/2}$$

and

$$J(E_e > 31 \text{ MeV}) = 9.9 \times 10^7 \exp(-L/1.51) \left(\frac{\cos^6 \Lambda}{\sqrt{4 - 3 \cos^2 \Lambda}} \right)^{m/2}$$

with J the omnidirectional intensity in electrons/cm²-sec, L in units of R_J , and Λ the magnetic latitude in the dipolar model previously described. The values of m are given in the previous paragraph for C and D, respectively.

A simple power law of the form $dJ/dE \propto E_e^{-\gamma}$ was determined for detectors C and D. The values of γ are plotted as a function of L in Figure 11. The data track very well inbound and outbound from $L = 3.4$ to $L = 14$. Beyond L of 14, statistical fluctuations in the counting rate produce much scatter. Inside L of 3.4, the slightly different angular distributions produce different values of γ for different magnetic latitudes.

Taking a mean value of $\gamma = 3.5$ and the two curves of Figures 9 and 10 one obtains a mean equatorial differential energy spectrum for electrons with energy greater than 21 MeV of

$$\frac{dJ}{dE} \approx 1.4 \times 10^{12} E^{-3.5} \exp(-r/1.45) \text{ cm}^2\text{-sec-MeV} \quad .$$

The outbound dip in intensity centered at $L = 15 R_J$ shown in all figures is attributed to Ganymede. On the inbound passage the spacecraft was very near the equator (see Figure 14) while Ganymede would have had an immediate effect on particles on the same field

line if they mirrored at greater than 8.9° magnetic latitude. On the outbound pass the situation was quite different. The spacecraft crossed its orbit at about 22° magnetic latitude while Ganymede would have affected particles mirroring at greater than 9.2° magnetic latitude on the same field line. The time of this crossing would have been six hours before. The $\bar{E} = 0$ drift periods for 21 MeV and 31 MeV electrons are 7.3 and 5 hours, respectively, at this radial distance, but Ganymede crossed the magnetic equator during the ~~inbound~~ thereby eliminating even the drifting particles. Other satellite crossings show no discernible effect on detectors C and D as is evidenced by Figure 9 and 10.

The following table gives the magnetic latitude of the Pioneer spacecraft at the satellite orbit crossing as well as the magnetic latitude of the satellite and time delay when the satellite crossed the same field line that the spacecraft should have observed. The $\bar{E} = 0$ drift period of 21 MeV electrons at each satellite orbit is also indicated. This table and Figures 13 and 14 give a good view of the geometry of the crossings.

	Io		Europa		Ganymede	
	<u>in</u>	<u>out</u>	<u>in</u>	<u>out</u>	<u>in</u>	<u>out</u>
Magnetic Latitude of Pioneer 10	-5.9°	14.4°	-17.6°	5.0°	-1.7°	22.0°
Magnetic Latitude of Satellite	7.6	1.2°	5.0°	-8.3°	8.9	9.2°
Time Delay in Hours	1.8	5.6	10.5	4.0	0.7	6.2
Drift Period for 21 MeV Electrons in Hours	18.6		11.7		7.3	

The table makes it evident that the most noticeable effects should occur at the Europa crossing inbound and at the Io and Ganymede crossings outbound.

Figure 12 shows the counting rates observed by detectors G, B, A, C, and D of the University of Iowa instrument on board Pioneer 10 when the spacecraft was within $20 R_J$ of the planet. All detectors show similar behavior at the outbound Ganymede crossing. Detectors G and B show definite dips at the inbound crossing of Europa orbit. A slight dip is noticeable at the outbound Io orbit in the rates of B, G, and A.

The inbound Ganymede and outbound Europa crossings show up in Figure 12 as possible turbulent wakes in the low-energy particles caused by the passage of the satellite. A thorough analysis of the satellite crossings has not been done, but it would have to be based on a theoretical formulation of combined radial and pitch angle diffusion. The theoretical framework for this has been developed [Roederer, 1970] but to our knowledge no comprehensive calculations have been completed even for the earth's magnetosphere.

The energetic electron ($E > 21$ MeV) observations indicate that they must radially diffuse very rapidly. That is, they are able to pass the orbit of the satellite in less than the rotation period of Jupiter. The pitch angle diffusion must also take place on the same time scale, since the sweeping effect of the satellites and the drift periods of the electrons limit the replacement time, yet

the equatorial angular distribution appears to be proportional to $\sin^4 \alpha$.

The detailed analysis such as Figures 9 and 10 for detectors G, B, and A to find the equatorial intensities, angular distributions, and satellite effects is not yet completed. Since these detectors are directional it is necessary to de-convolve the look angle distribution and with the orientation of the spacecraft and the magnetic field model, to determine the local pitch angle distribution.

V. THE MAGNETODISC

The region outside $20 R_J$, referred to as the magnetodisc, was previously characterized as a region of quasi-trapped particles. The initial observations shown in Figure 15 lead one to speculate that the magnetospheres of the earth and Jupiter are similar with a bow shock, magnetosheath, magnetopause, and so on, but only on a much larger scale. Figure 16 shows that this is not the case; specifically, the particle intensities show a 10-hour periodicity in amplitude superimposed upon a gradual increase in magnitude.

The drop-out of particle intensity on December 1 is the most unusual feature of the inbound data. The plasma analyzer experimenters [Wolf et al., 1974] suggest that a impulsive increase in solar wind pressure caused an inward movement of the sunward magnetopause. If this were the case, the particle detectors should have shown evidence of previously observed intensities. Instead the particle intensity became very low, while the scalar value of the magnetic field remained the same as before. For more discussion of this phenomena it is desirable to investigate the post-encounter data.

Figure 17 shows very sharp modulations in intensity with a 10-hour periodicity out to about 80 Jovian radii. Beyond this distance the periodicity becomes more erratic but intensity variations continue (Figure 18) out to almost 175 Jovian radii.

A determination of the System III longitude of the intensity maxima for the outbound data shows a spiraling of the apparent location of the longitude of the dipole tilt. A good fit of the peak intensities for the outbound data was obtained using a centered dipole with a tilt of 9.5° towards 230° longitude out to $30 R_J$. Beyond this point, the data could be fit if the apparent longitude of the dipole were decreased from 230° by the following function of radius:

$$3.67 \exp (R/24.6) \quad .$$

This organizes the data out to about $80 R_J$ into a thin ($< 5 R_J$) disc-like structure.

The inbound maxima show a completely different story: The apparent longitude of the dipole tilt seems to be constant at value slightly greater than 230° out to $70 R_J$. The exception to this occurs for the two maxima after the data drop-out on December 1. Here the apparent longitude of the dipole tilt is shifted to 260° .

This suggests another possible interpretation for the data drop-out, that the Pioneer 10 spacecraft observed a breaking and reconnection of field lines. The breaking resulted in the loss of particles and the subsequent reconnection explains the momentary forward shift of the apparent dipole longitude.

ACKNOWLEDGMENTS

I would like to thank Dr. J. A. Van Allen and Mr. D. N. Baker and Mr. D. D. Sentman for allowing this work to be presented prior to more complete joint publication [Van Allen et al., 1974b].

The handling of the Pioneer 10/11 program by the Ames Research Center is gratefully acknowledged.

The project manager for development of the University of Iowa instrument is Roger F. Randall, who designed and developed all the electronics and supervised all engineering aspects. Others at the University of Iowa to whom I am especially indebted are D. E. Cramer, H. D. Owens, R. B. Brechwald, R. J. France, M. Thomsen, and H. R. Flindt.

This work has been supported by Contracts NAS2-5603 and NAS2-6553 with the Ames Research Center of the National Aeronautics and Space Administration and by Contract N00014-68-A-0196-0009 with the Office of Naval Research.

REFERENCES

- Carr, T. D., and S. Gulkis, The magnetosphere of Jupiter, Annual Review of Astronomy and Astrophysics, 7, 577-618, 1969.
- Chang, D. B., and L. Davis, Jr., Synchrotron radiation as the source of Jupiter's polarized decimetric radiation, Astrophys. J., 136, 567-581, 1962.
- Mead, G. D., Magnetic coordinates for the Pioneer 10 Jupiter flyby, Unpublished Memorandum, Goddard Space Flight Center, April 1973.
- McIlwain, C. E., Coordinates for mapping the distribution of magnetically trapped particles, J. Geophys. Res., 66, 3681-3691, 1961.
- Ortwein, N. R., D. B. Chang, and L. Davis, Jr., Synchrotron radiation from a dipole field, Astrophys. J. Suppl. Series, Vol. 12, 323, 1966.
- Roederer, J. G., Dynamics of Geomagnetically Trapped Radiation, Springer-Verlag, New York, Heidelberg, Berlin, 1970.
- Smith, E. J., Memorandum to Pioneer Particle Investigators, May 13, 1974.

- Smith, E. J., L. Davis, Jr., D. E. Jones, D. S. Colburn, P. J. Coleman, Jr., P. Dyal, and C. P. Sonett, Magnetic field of Jupiter and its interaction with the solar wind, Science, 183, 305-306, 1974.
- Thomsen, M. F., The heliocentric radial cosmic ray gradient, M.S. Thesis, University of Iowa, May 1974.
- Thorne, K. S., The theory of synchrotron radiation from stars with dipole magnetic fields, Astrophys. J. Suppl., 8, 1-30, 1963.
- Thorne, K. S., Dependence of Jupiter's decimeter radiation on the electron distribution in its Van Allen belts, Radio Science, 69-D, 1557, 1965.
- Van Allen, J. A., Initial flight report on University of Iowa experiment on Pioneer 10, University of Iowa Research Report 72-5, March 27, 1972.
- Van Allen, J. A., Observations of Galactic Cosmic-Ray Intensity at Heliocentric Radial Distances from 1.0 to 2.0 Astronomical Units, Astrophys. J., 177, L49-L52, 1972.
- Van Allen, J. A., D. N. Baker, B. A. Randall, M. F. Thomsen, D. D. Sentman, and H. R. Flindt, Energetic electrons in the magnetosphere of Jupiter, Science, 183, 309-311, 1974a.
- Van Allen, J. A., D. N. Baker, B. A. Randall, and D. D. Sentman, The magnetosphere of Jupiter as observed with Pioneer 10. Part I: Instrument and principal findings, accepted by J. Geophys. Res., 1974b.

Van Allen, J. A., L. A. Frank, and B. J. O'Brien, Satellite
observations of the artificial radiation belt of July
1962, J. Geophys. Res., 68, 619-627, 1963.

Wolfe, J. H., H. R. Collard, J. D. Mihalov, and D. S. Intriligator,
Preliminary Pioneer 10 encounter results from the Ames
Research Center plasma analyzer experiment, Science, 183,
303-305, 1974.

CAPTIONS FOR FIGURES

- Figure 1. Cut-away view of one system of detectors. A, C, and B are miniature, end-window EON 6213 Geiger-Mueller tubes. The Z-axis is parallel to the rotational axis of the spacecraft.
- Figure 2. Cross-sectional view of the heavily shielded triangular array of miniature, cylindrical EON 5107 Geiger-Mueller tubes D, E, and F.
- Figure 3. Cut-away view of the arrangement of the single EON 6213 Geiger-Mueller tube G. Low-energy particles enter the end-window of the tube only after being scattered from the inner walls of the gold-plated elbow.
- Figure 4. Sketch of the overall configuration of the University of Iowa instrument.
- Figure 5. Inbound and outbound counting rates of detector C ($E_e > 21$ MeV) as a function of L for the Smith et al. [1974] model of the Jovian magnetic field. All rates are corrected to magnetic equatorial values assuming a pitch angle distribution $j \propto \sin^4 \alpha$.
- Figure 6. A plot similar to Figure 5 but for a centered dipole, tilted at 9.5° towards 230° System III longitude.
- Figure 7. A plot similar to Figure 5 but with a newer magnetic model by Smith et al. [1974].

Figure 8. Inbound and outbound raw counting rate of detector C

($E_e > 21$ MeV) as a function of L for centered dipole, tilted at 9.5° toward 230° System III longitude, show the exponential behavior of the equatorial particle intensities.

Figure 9. An improved version of Figure 6, assuming a simple L-dependence of m in the angular distribution $j \propto \sin^m \alpha$.

Figure 10. A plot similar to Figure 9 for detector D ($E_e > 31$ MeV).

Figure 11. The L-dependence of the differential spectral index γ in a power law spectrum as derived from the counting rate ratio C/D. The abscissa is based on a 9.5° tilt of the dipole toward System III longitude = 230° .

Figure 12. The counting rates of particles observed by detectors G, B, A, C, and D in the inner magnetosphere of Jupiter. The radial distance in Jovian radii and approximate satellite location are indicated.

Figure 13. Projection on the ecliptic plane of the hyperbolic encounter trajectory of Pioneer 10 and the orbits of the four inner Jovian satellites. The numbers 1 and 2 on the orbits of JI, JII, and JIII show the positions of each of these satellites at the time that the spacecraft crossed the L-shell of that satellite, inbound and outbound, respectively. The number 3 shows the position of JV at the time that the spacecraft was at periapsis, marked P. $\gamma_{\mathcal{U}}$ designates Jupiter's vernal equinox and γ_{\oplus} designates Earth's vernal

equinox. The ephemerides are courtesy of M. Helton of the Jet Propulsion Laboratory. Note that the spacecraft spin axis is parallel to the planet-earth line throughout the encounter.

Figure 14. The time-labeled trace of Pioneer 10 in magnetic polar coordinates (magnetic meridian plane projection) for the planetary dipolar model as specified. The cross-hatching shows the regions that bound the orbits of Io (JI), Europa (JII), and Ganymede (JIII), respectively, in such a coordinate system.

Figure 15. Detailed magnetic field strength and electron intensity data associated with the crossing of the bow shock and magnetopause.

Figure 16. Seven days of observations on the inbound leg of the encounter trajectory through the sunward portion of the magnetodisc.

Figure 17. Six days of observations on the outbound leg of the encounter trajectory through the pre-down portion of the magnetodisc.

Figure 18. Six further days of observations on the outbound leg of the encounter trajectory through the pre-down portion of the magnetodisc.

A-G70-316-1

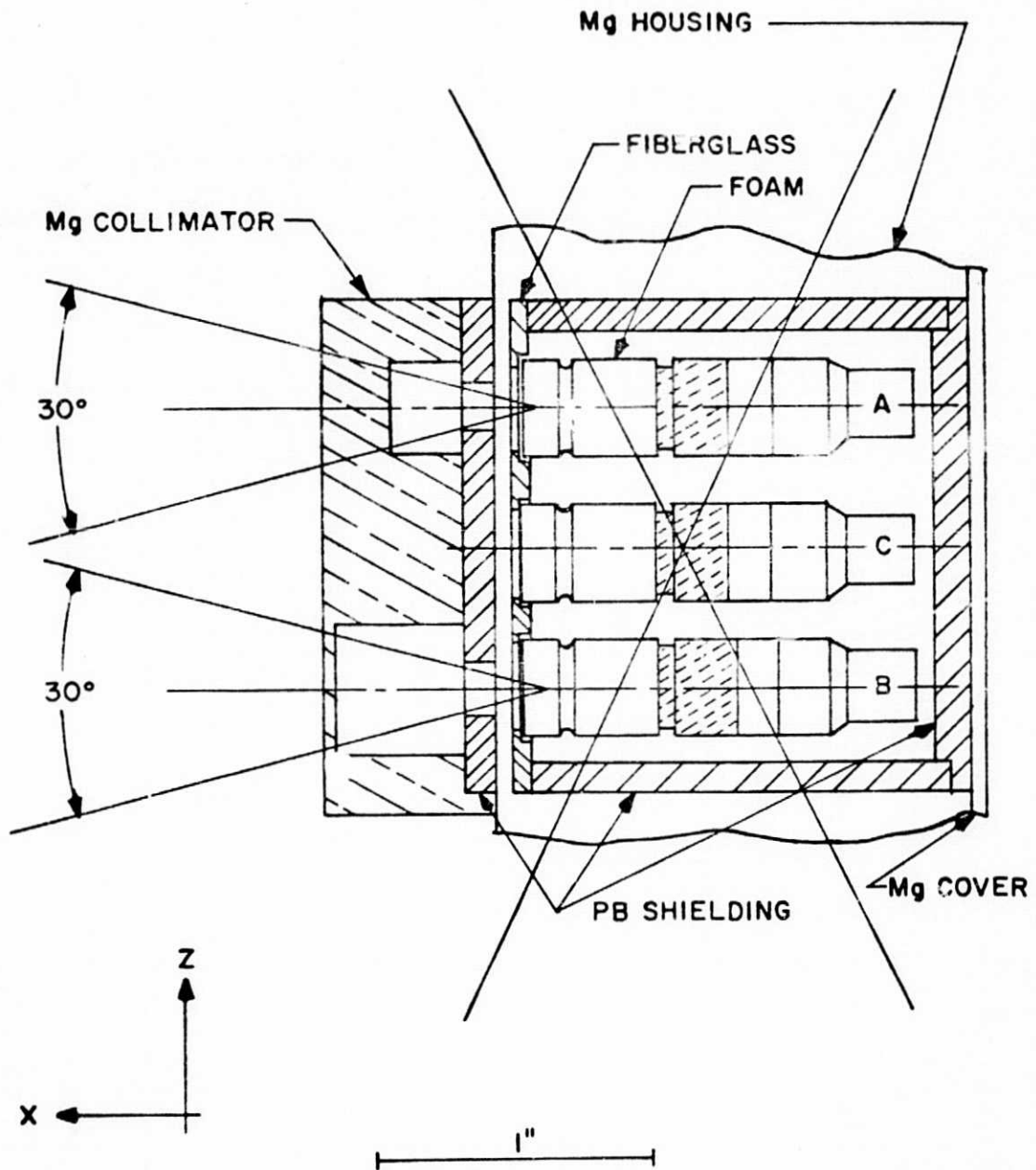


Figure 1

A-G69-677

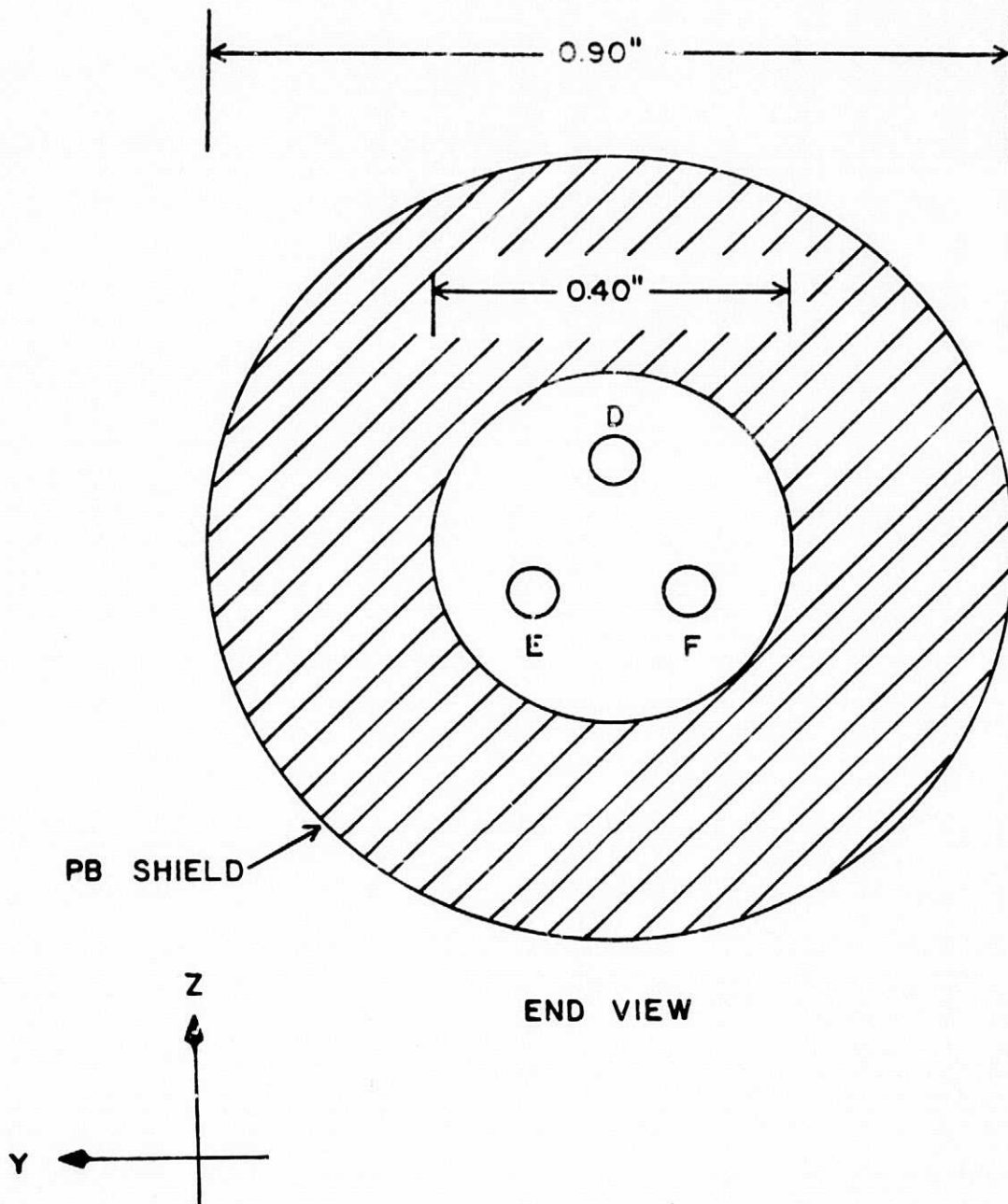


Figure 2

A-G70-592-1

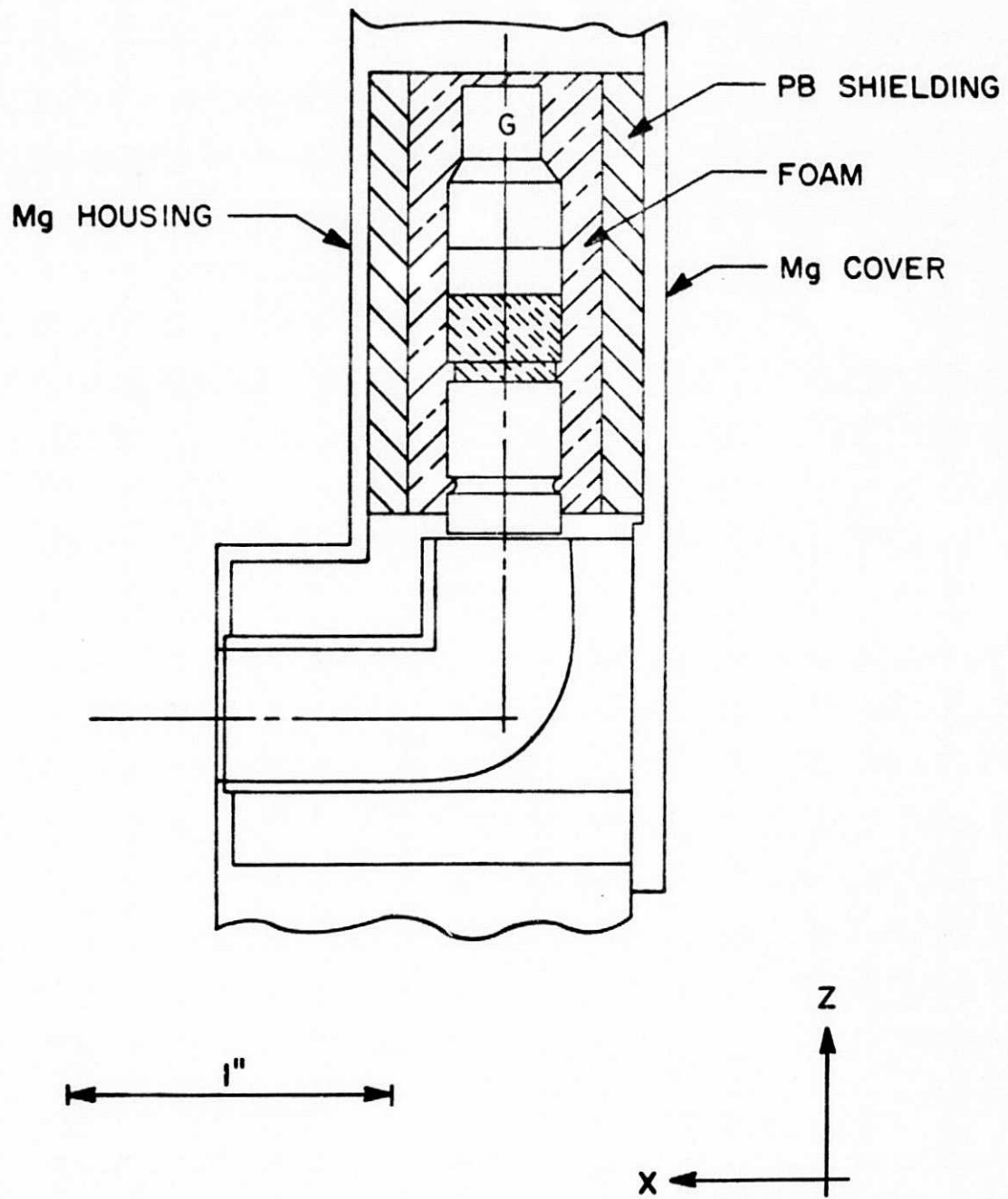


Figure 3

A-G71-78

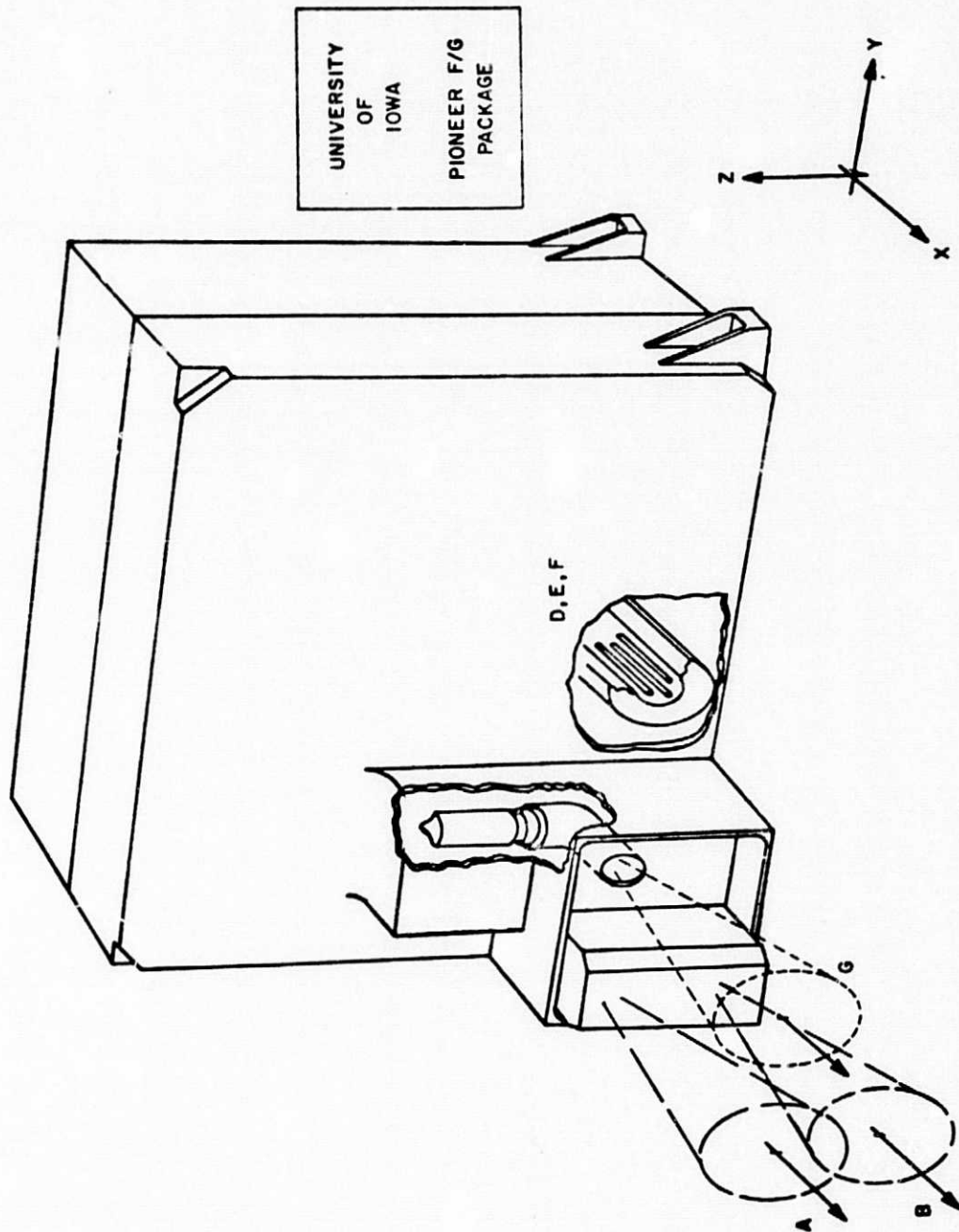


Figure 4

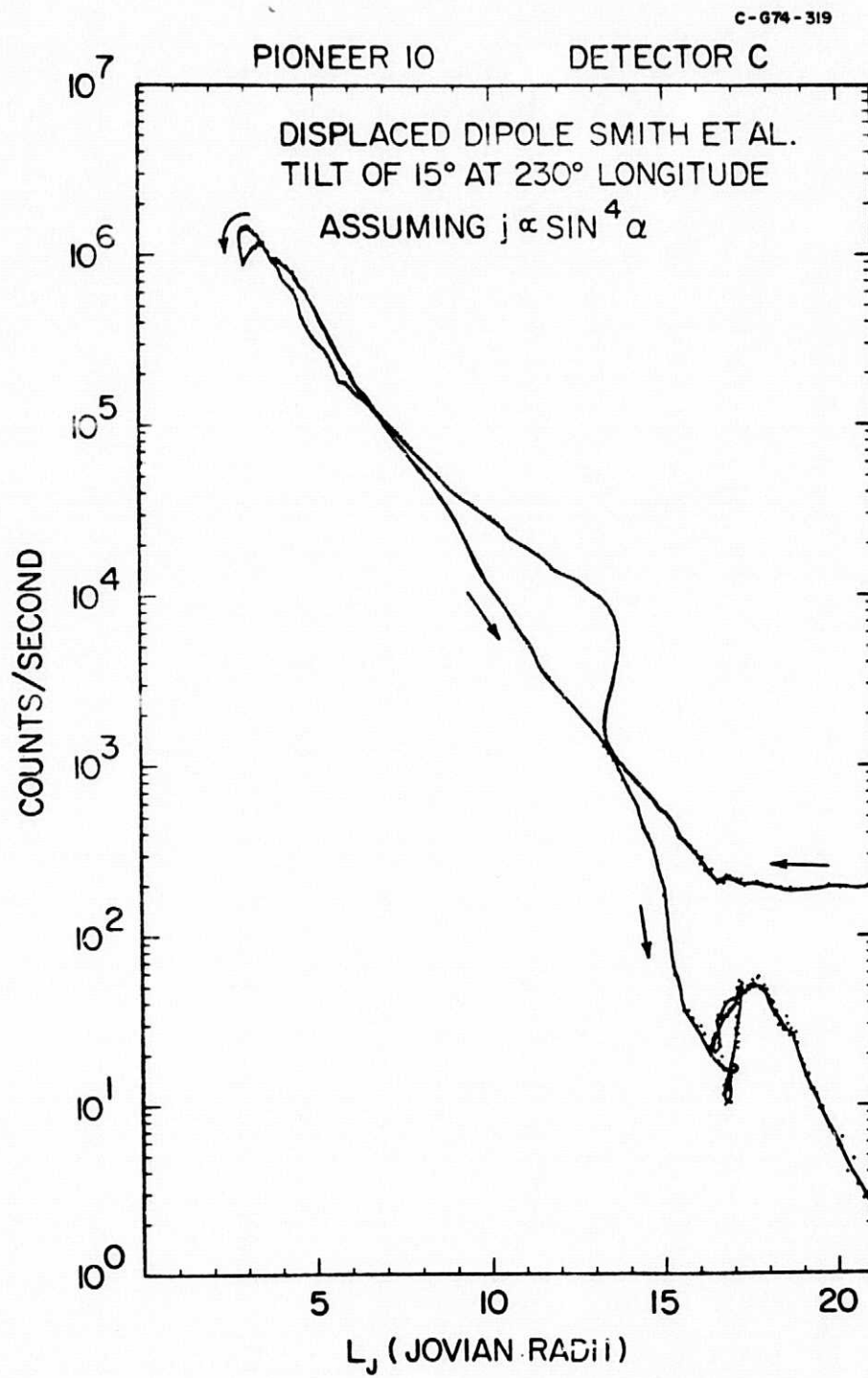


Figure 5

C-674-316

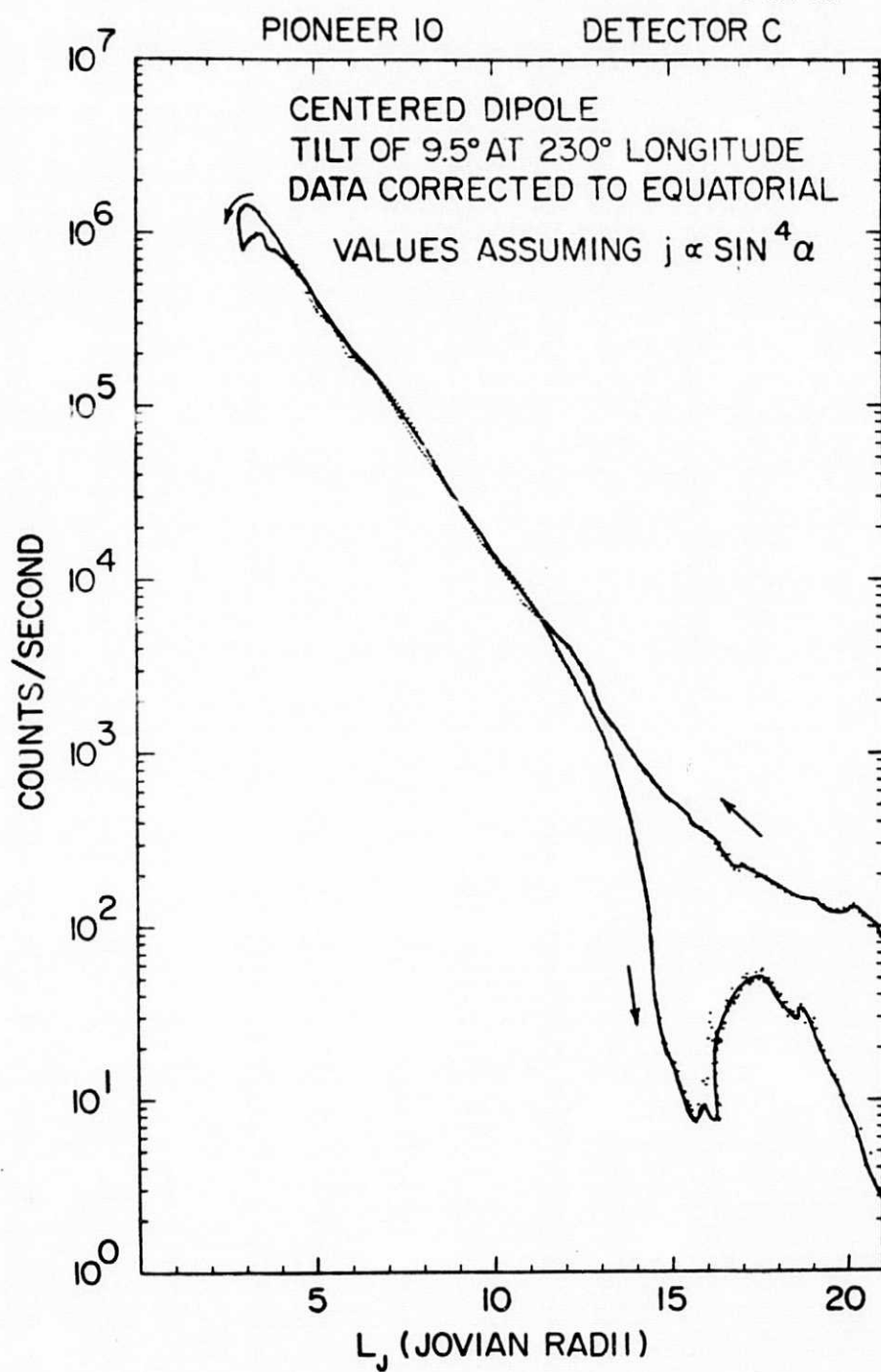


Figure 6

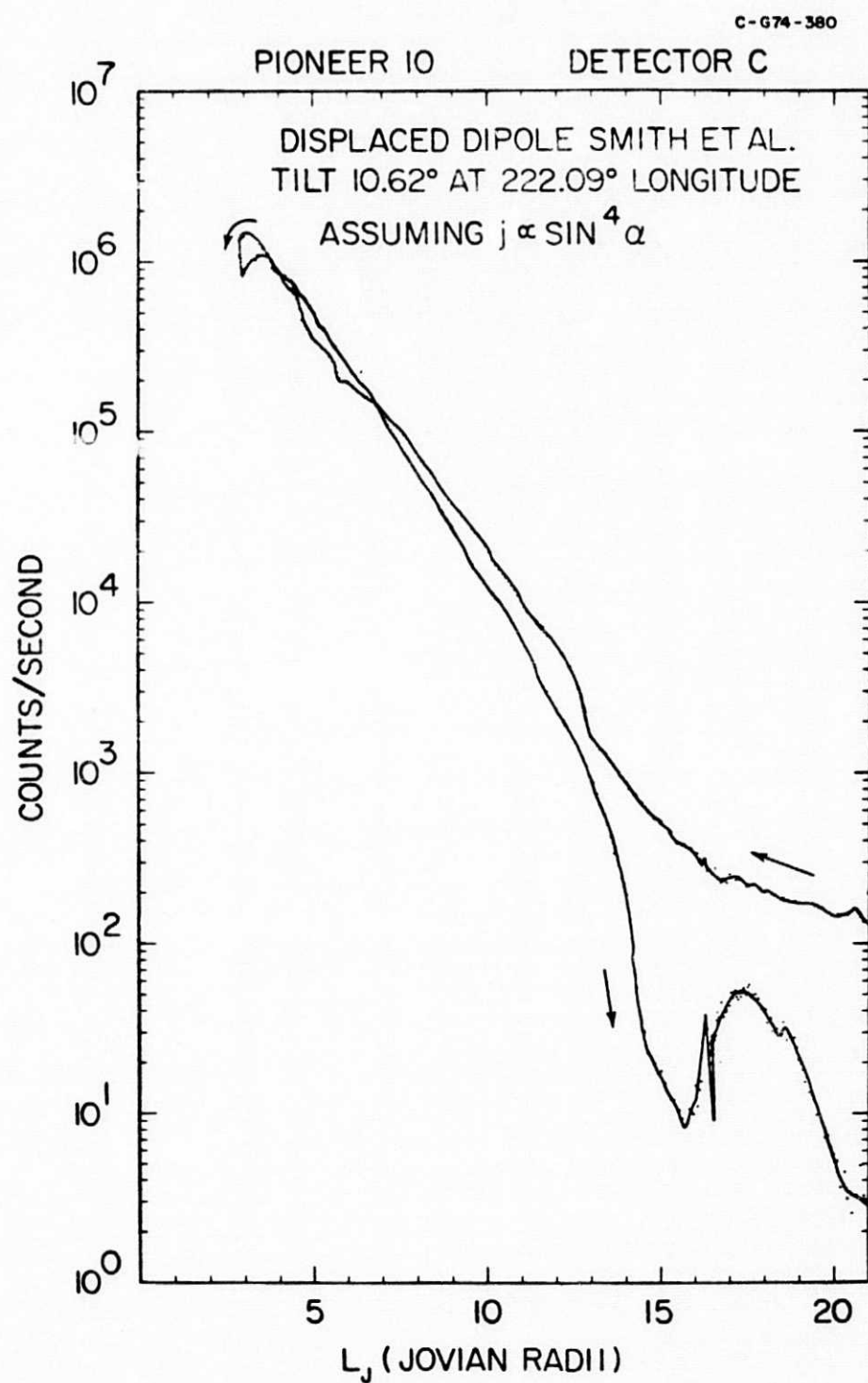


Figure 7

C-674-317

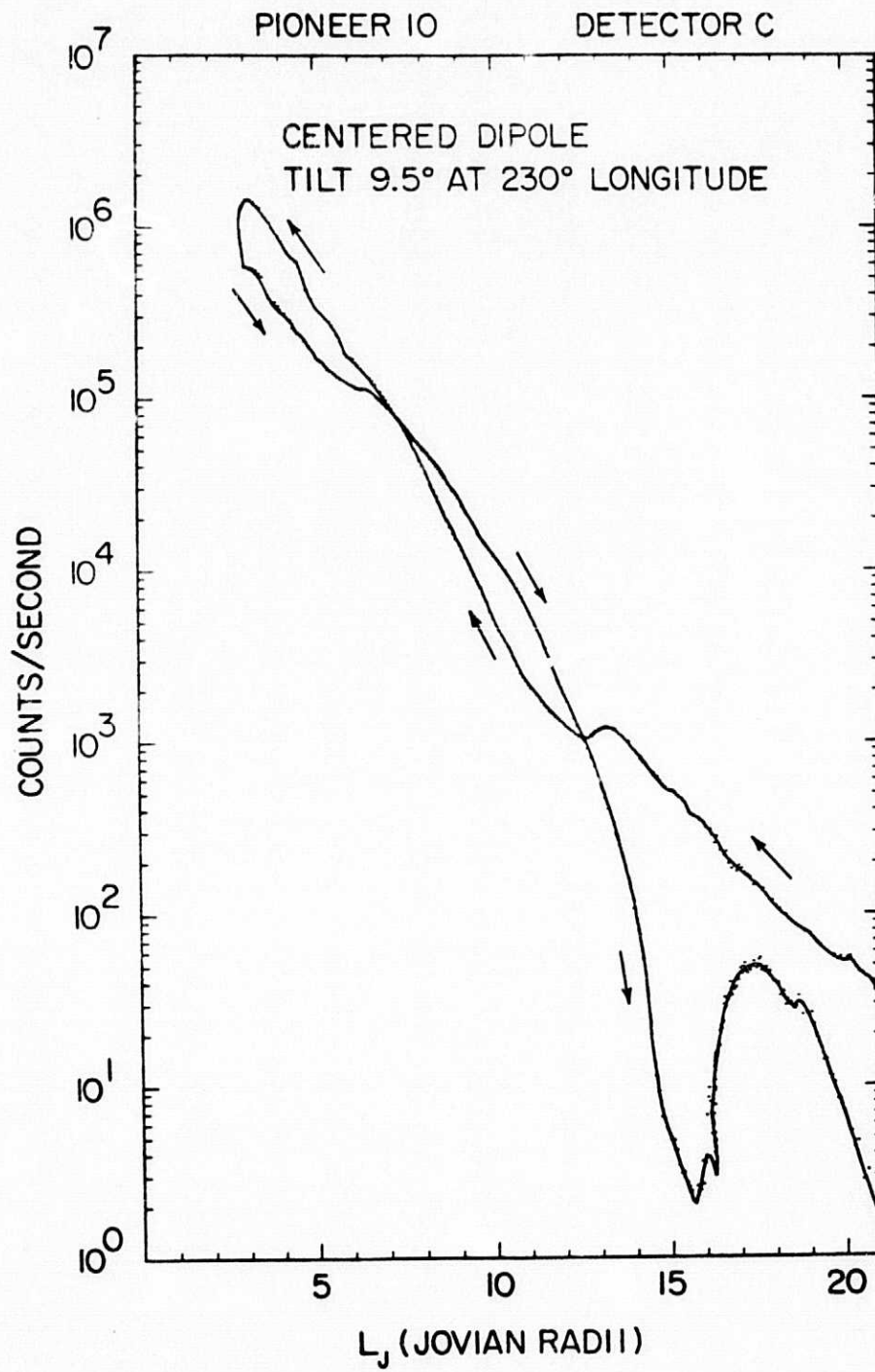


Figure 8

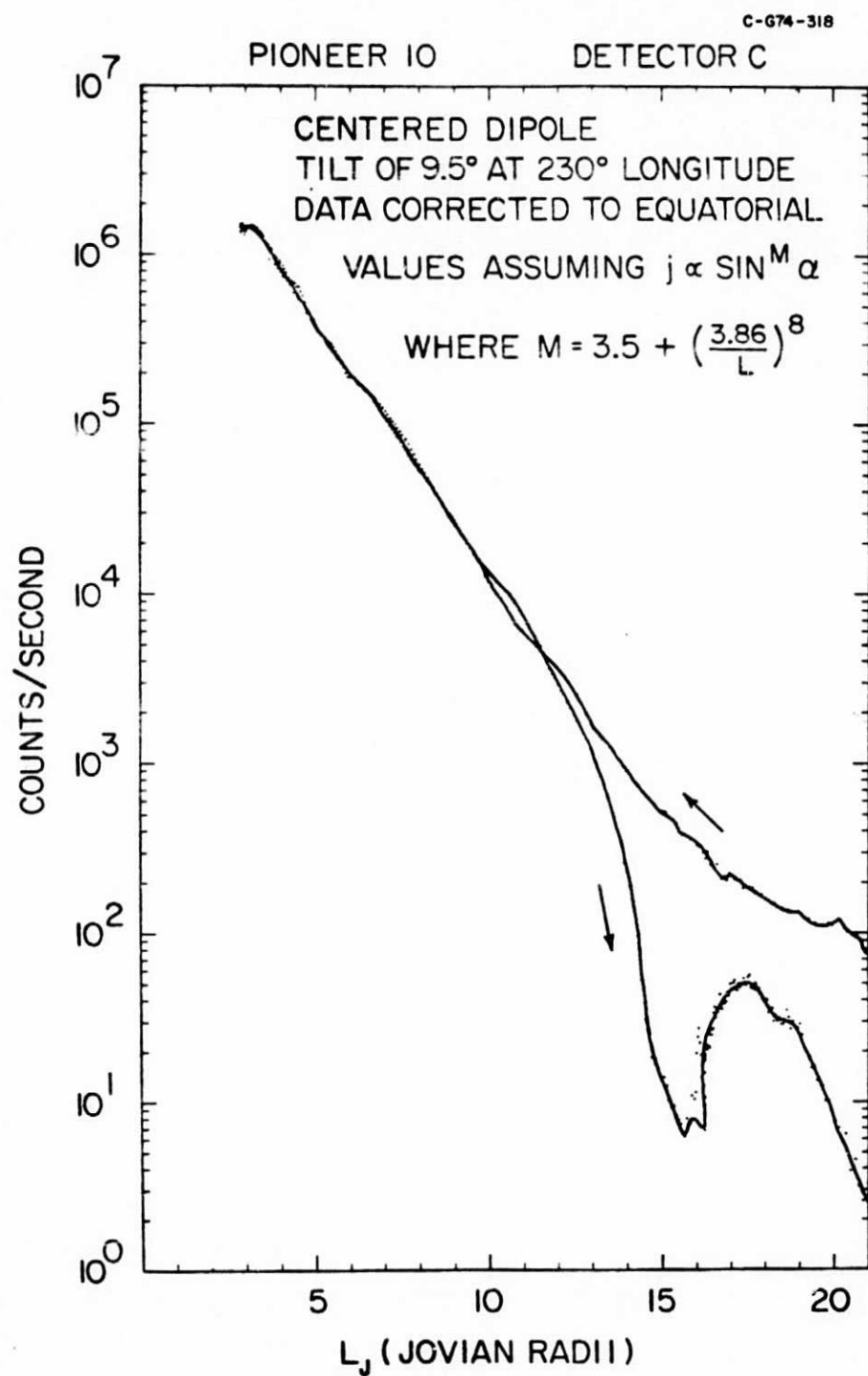


Figure 9

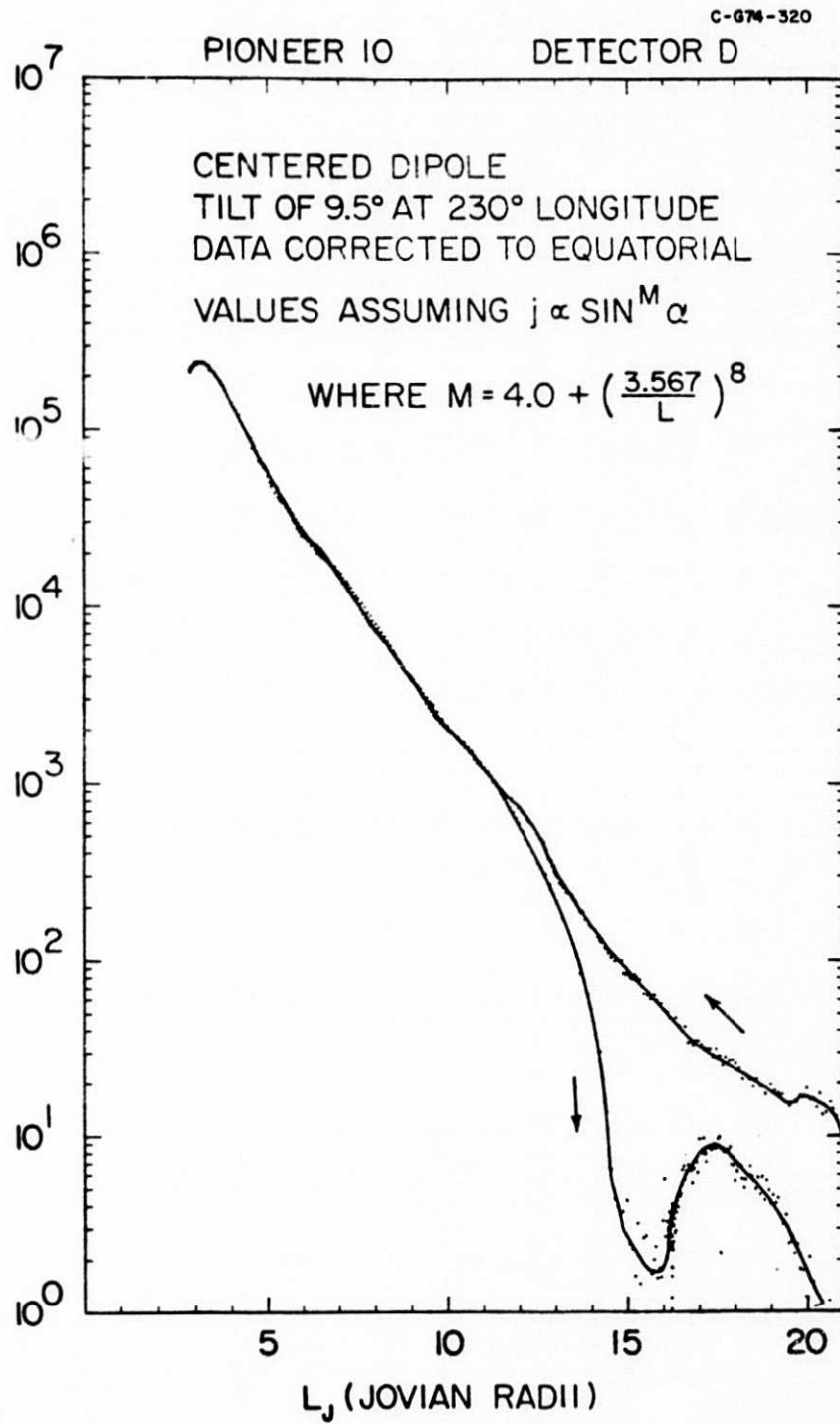


Figure 10

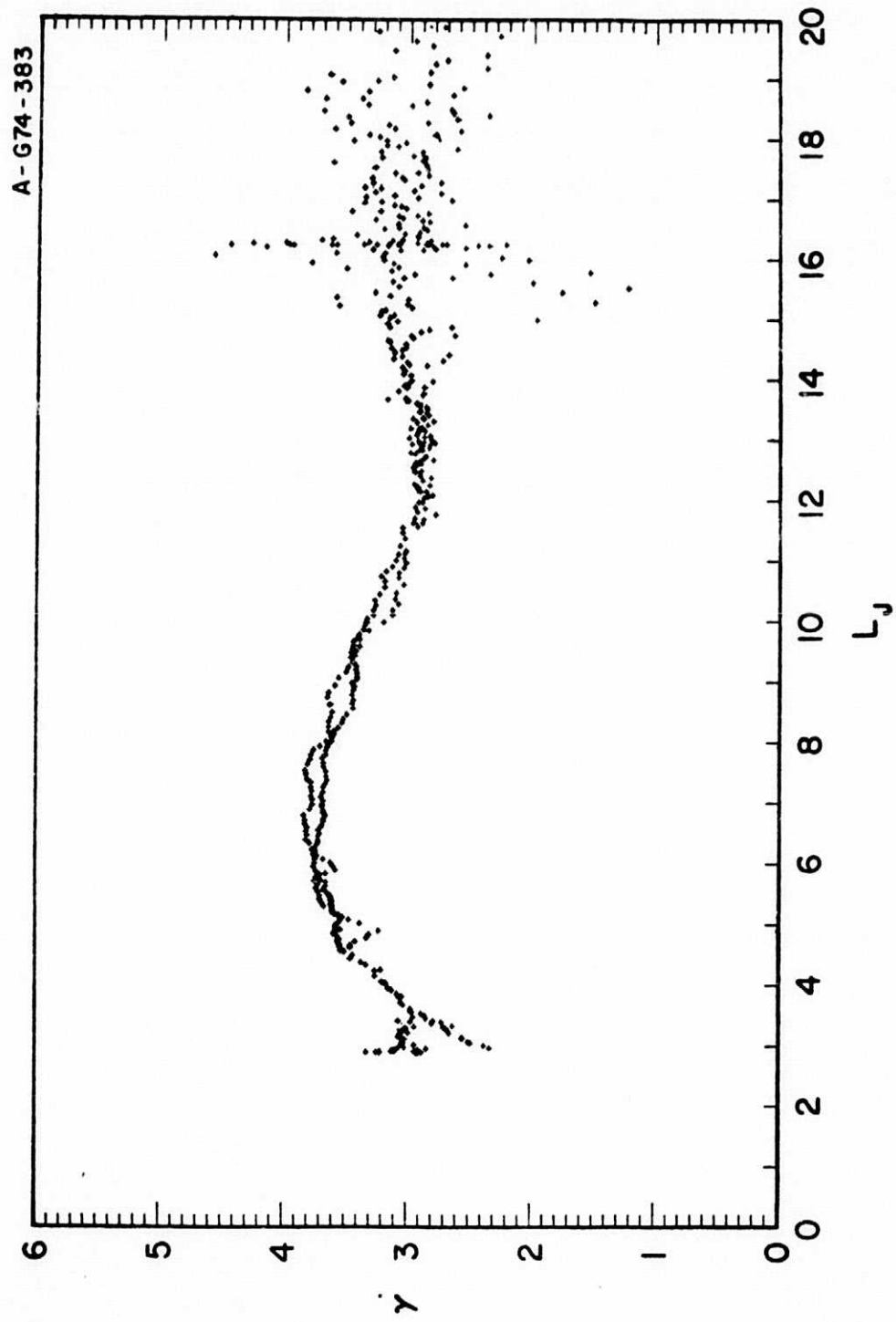


Figure 11

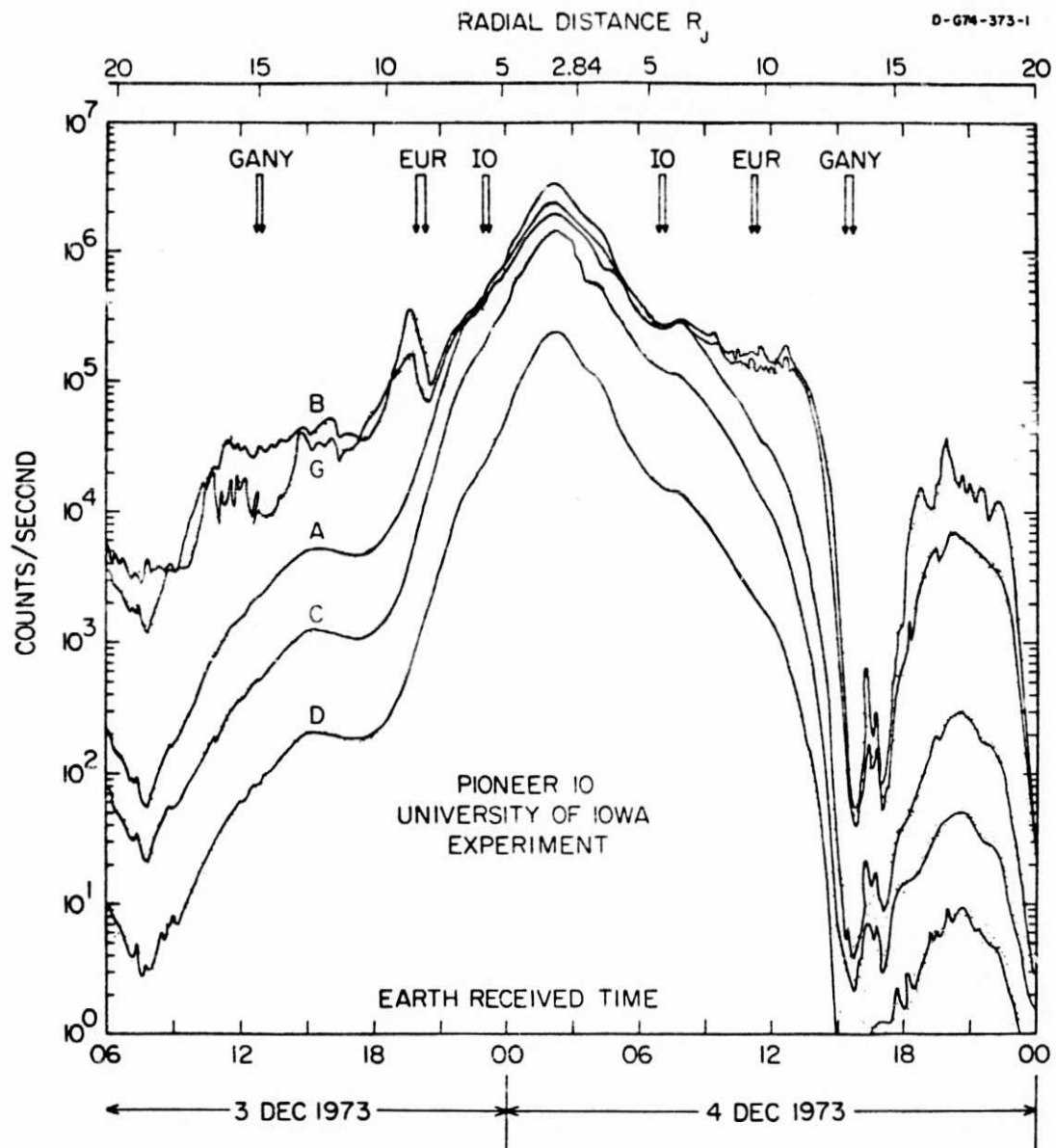


Figure 12

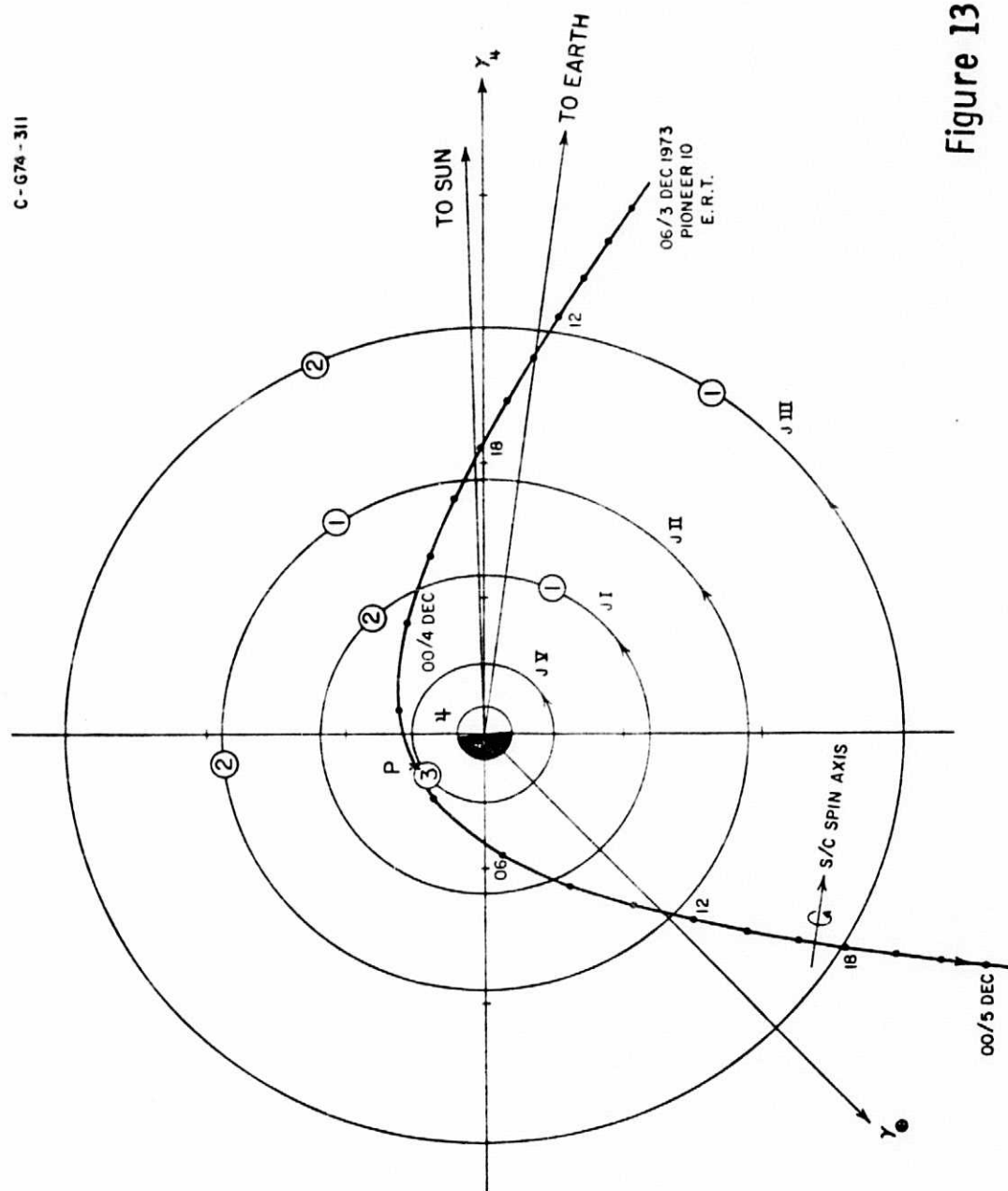


Figure 13

D-GM-326

PIONEER 10 ENCOUNTER
MAGNETIC MERIDIAN PLANE PROJECTION

CENTERED DIPOLE $\left\{ \begin{array}{l} \text{TILT} = 9.5^\circ \\ \lambda_{III} (1957) = 230^\circ \end{array} \right.$

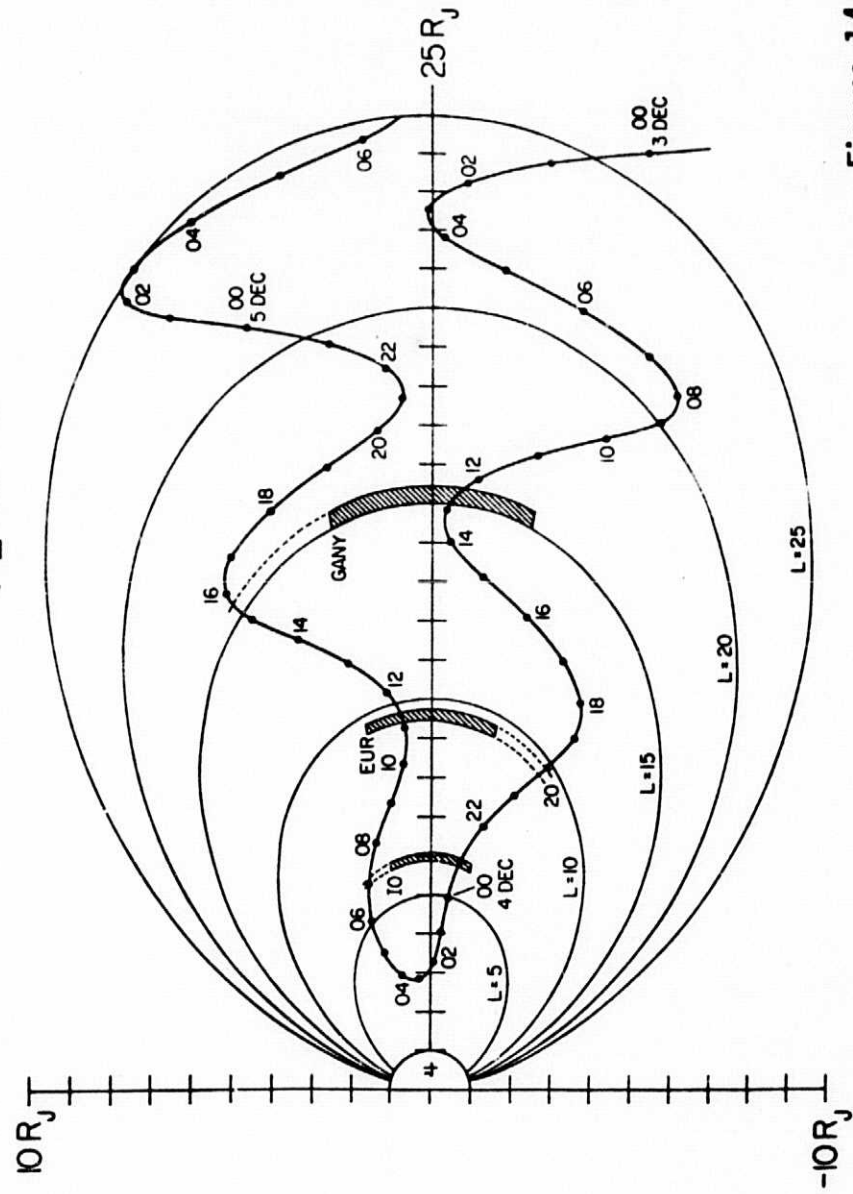


Figure 14

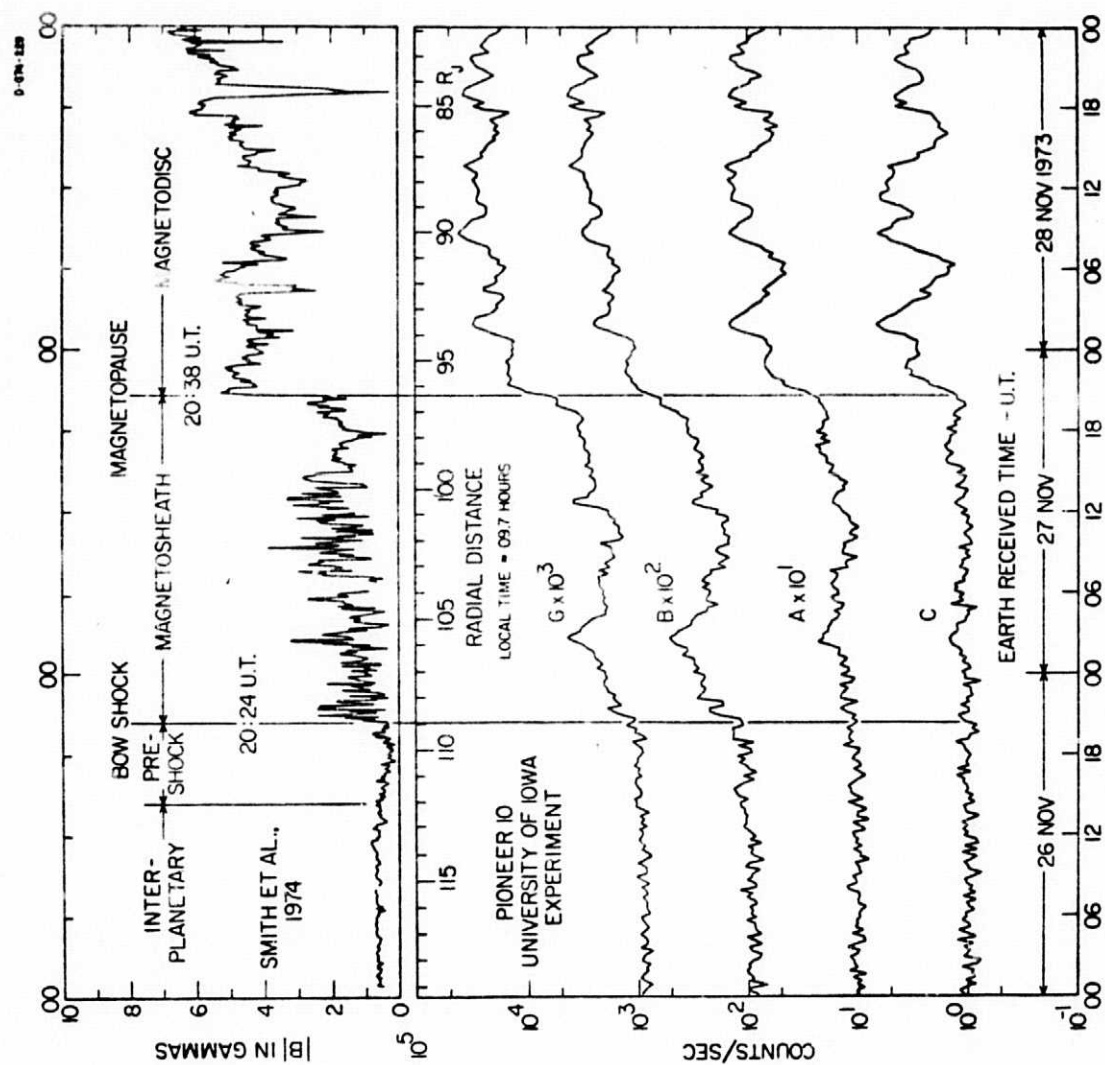


Figure 15

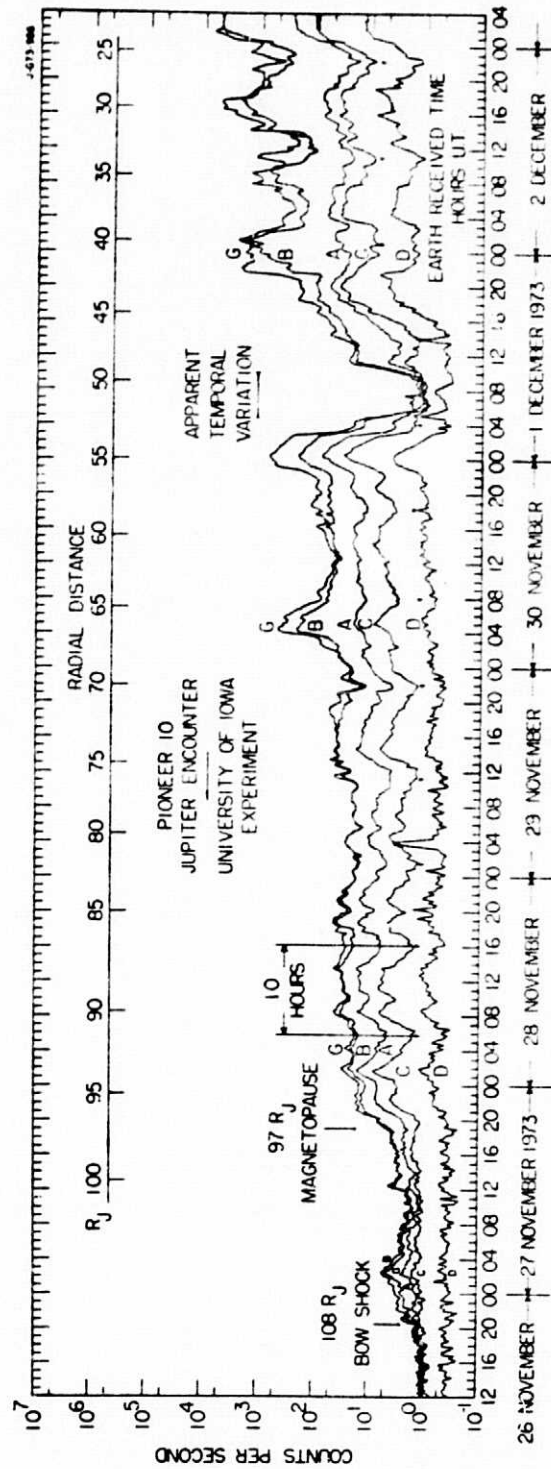


Figure 16

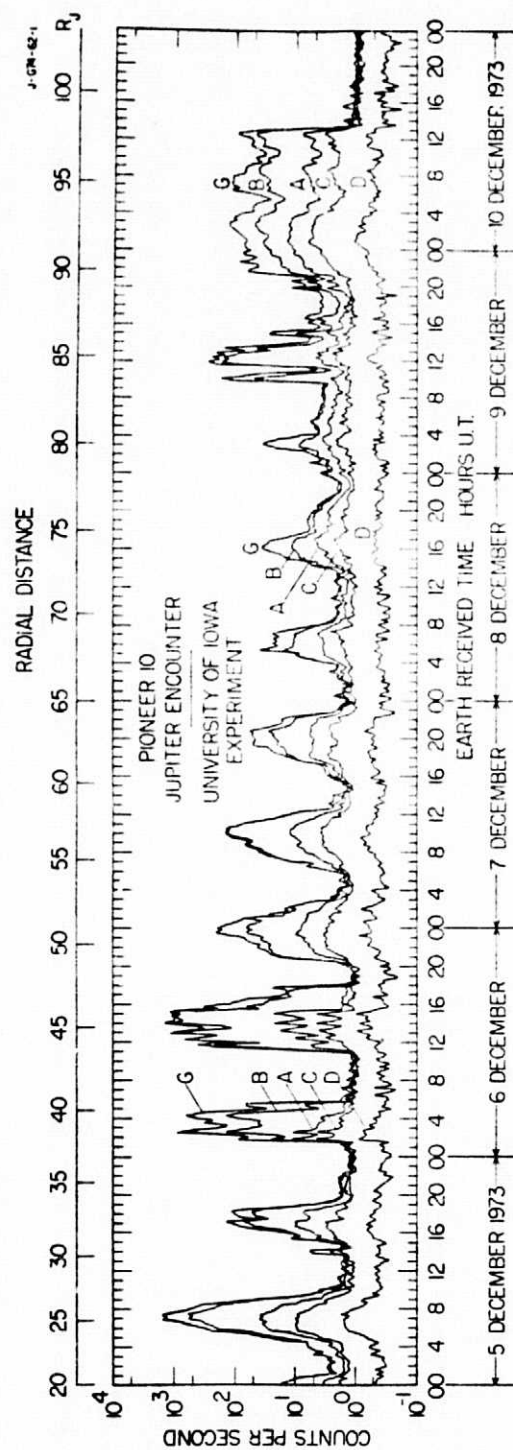


Figure 17

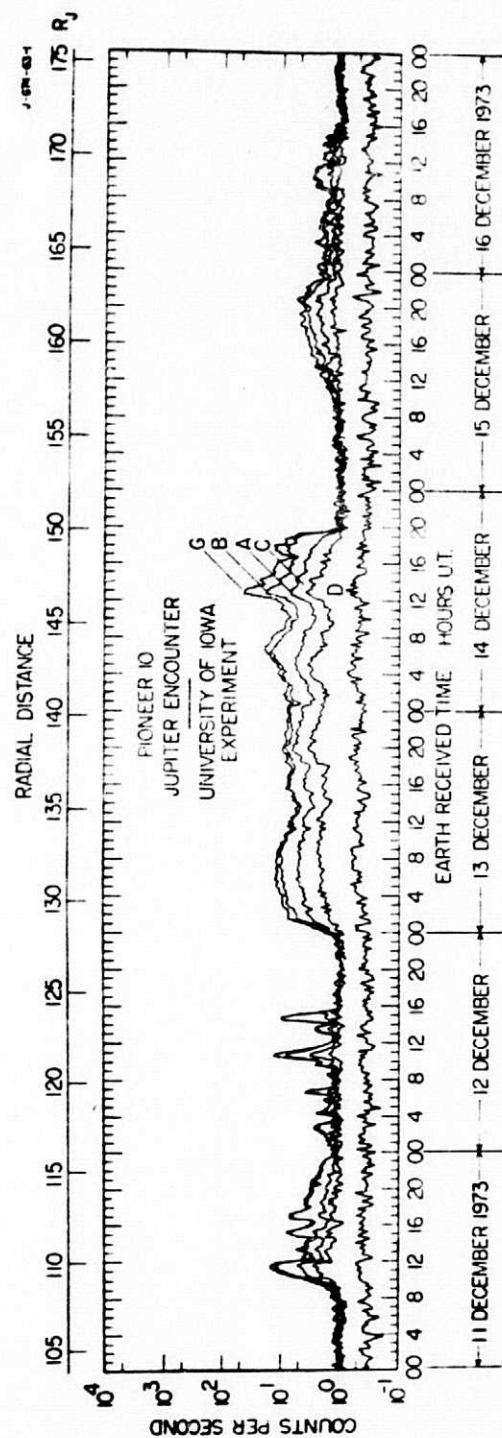


Figure 18